Performance analysis of propeller configurations: a study on blade diameter, pitch, and number of blades for optimal thrust

Nkosingiphile Langa[1*], *Riaan* Stopforth[1], *Daniel* Kirkman[2] and *Maxim* Buzdalov[3]

[1]Scientific Multidisciplinary Advanced Research Technologies (SMART) Lab, University of KwaZulu-Natal, KwaZulu-Natal, South Africa
[2]Department of Mechanical Engineering, University of KwaZulu-Natal, KwaZulu-Natal, South Africa
[3]Department of Computer Science, Aberystwyth University, United Kingdom

Abstract. Optimising thrust generation is fundamental to enhancing the performance, efficiency, and manoeuvrability of unmanned aerial vehicles (UAVs), especially as their applications expand across diverse sectors. This paper presents a performance analysis of propeller configurations, investigating the effects of blade diameter, pitch, and blade count on thrust output. Utilising a custom-built, low-cost frictionless test rig, a systematic approach evaluated various configurations under controlled conditions. The results show how each factor influences performance and provides practical advice for improving UAV designs.

1 Introduction

The rapid development of unmanned aerial vehicles (UAVs) has revolutionized industries ranging from logistics and surveillance to agriculture and disaster response. A crucial aspect of their performance is their propulsion system, which directly influences efficiency, thrust generation, and flight stability [1]. For UAVs to meet the demands of precision, endurance, and power efficiency, understanding and optimizing their propeller configurations is not just advantageous, it is imperative.

The selection and use of propellers are typically driven by their influence on the performance of various metrics such as thrust, efficiency, and energy consumption [2], [3]. Propellers are identified by three key parameters: diameter, pitch, and blade count. The pitch significantly impacts thrust and efficiency, with higher-pitch propellers producing greater thrust but at the cost of higher power consumption. Conversely, lower-pitch propellers offer better stability and efficiency at lower speeds, making pitch a critical parameter in propeller selection [4]. Blade count also affects propeller efficiency and noise [5]. Two-blade propellers are approximately 4% more efficient than three-blade counterparts of the same pitch and diameter [6]. This makes two-blade configurations preferable in scenarios prioritizing energy conservation. However, three-blade propellers, though less efficient,

* *Nkosingiphile* Langa: nkosingiphilekarllanga@gmail.com

provide increased thrust and are often used for high-power or turbulence-prone applications [6, 7].

When utilized in a prototype, contra-rotating or coaxial propellers are sometimes a preferable setup since they can potentially increase the net thrust and propulsion efficiency at higher speeds than single propellers [8]. By placing one propeller above or below another with an opposing rotational direction, airflow losses are reduced, thereby improving lift-to-drag ratios and overall performance [6]. Additionally, studies have shown that two-blade propellers with constant pitch often outperform three-blade variants regarding efficiency and power consumption [7].

These propellers are typically mounted on brushless direct current (BLDC) motors, which are preferred for UAV applications due to their high reliability, wide operational speed range, excellent torque control, low maintenance, and long lifespan (Hasilci and Mumcu, 2022). Electronic Speed Controllers (ESCs) regulate the speed of BLDC motors and are a critical component of modern propulsion systems [10]. User input is typically transmitted via 2.4 GHz radio frequency signals from a radio control (RC) transmitter to a connected receiver [11]. Most systems are powered by lithium-ion or lithium-polymer (LiPo) batteries, forming a purely electric and environmentally friendly propulsion solution [12].

This study explores the impact of propeller parameters, including blade diameter, pitch, and count, on thrust generation and UAV performance. By using a frictionless test rig and integrating components such as BLDC motors, ESCs, and LiPo batteries, the study evaluates how different configurations affect thrust generation, energy efficiency, and power consumption. Additionally, the performance of a constructed Ducted-Contra Rotating UAV is studied, varying the propeller parameters while keeping the diameter constant. The overarching goal is to provide practical insights that support the design and optimisation of UAV propulsion systems. It makes the following research contributions to UAV research and development:

- It develops and utilises a low-cost, replicable experimental setup (frictionless test rig) for evaluating UAV propulsion systems.
- It systematically analyses how variations in blade diameter, pitch, and blade count affect thrust, efficiency, and power consumption.
- It bridges the gap between theoretical specifications and real-world performance by validating optimal configurations through prototype testing.
- It identifies the most effective propeller configuration for thrust and energy efficiency in coaxial UAV designs.

The study is presented as follows: Section 2 describes the methodology, including the design and fabrication of the test rig, detailed specifications of the UAV propulsion system, and the testing procedure. Section 3 presents the results, comparing static thrust measurements and prototype performance outcomes using multiple propeller configurations. Section 4 concludes by highlighting the optimal configurations and suggesting areas for future work.

2 Methodology

While propeller configurations have been widely studied, this study takes a different approach by analysing them through experimental testing. It uses a low-cost test rig adapted from the DIY community and a UAV prototype belonging to the vertical take-off and landing (VTOL) tail sitter category, equipped with two contra-rotating propellers. The section presents the approach taken to carry out the two experiments, which will be referred to as the bench test and prototype test from this point forward.

2.1 Propulsion system architecture

The propulsion systems utilised in be bench test are different from those in the prototype test due to additional structures, components and procedures to analyse propellers in each case. A detailed description of the propulsion system is provided.

2.1.1 Bench test architecture

The bench test architecture consists of a frictionless test rig, fabricated from reused 20-mm PVC pipes and a 100 x 200 x 5 mm wooden board, incorporated with support components produced using fused deposition modelling (FDM) additive manufacturing. A 5 × 16 × 5 mm, C0-clearance deep-groove ball bearing (type 625) was press-fitted into the arm- support joint, and a GT2 Idler timing pulley was bolted to the 3D-printed pulley holder to guide the fishing line, thereby minimising friction in the support and across the rig. Figure 1 illustrates a schematic layout and the actual constructed test rig.

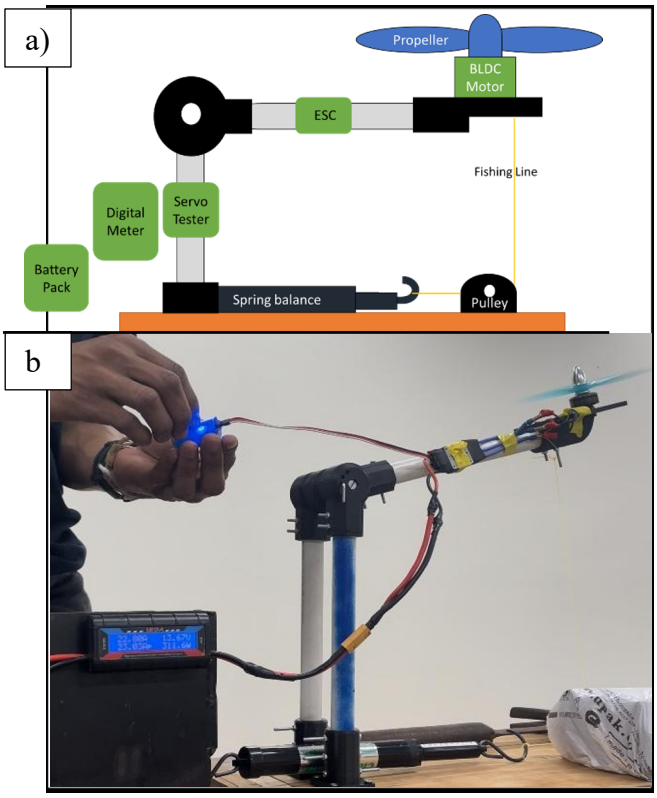

Fig. 1. Bench test architecture: a) layout of the test rig, b) the constructed test rig.

The thrust measuring instrument was a spring balance tied with a small fishing line, which was selected due to it being a low-cost practical and easily available solution. The selection of the hardware mounted on the rig was based on availability and overall compatibility to analyse propellers. The two brushless motors chosen were; the Aeolian Outrunner Brushless Motor C2830 1000 kv RC and the T-Motor F60PRO V2 1750 kv. These motors are highly recommended in RC plane construction and FPV drone racing community. Table 1 supplies more detailed specifications for each component.

From the available propellers, three were selected for testing based on compatibility with the BLDC motors. As shown in the manufacturer recommendations in Table 1, 5-inch, 8-inch, and 9-inch propellers were chosen. The BLDC motors were tested with two recommended ESCs—the 25 A and 30 A Aeolian units. A servo adjuster was used to regulate the input (acting similarly to a transmitter and receiver). Power for each test was supplied by either a 4S Nano-Platinum Series (14.8 V) or a 2S Turnigy (7.4 V) lithium-polymer (LiPo) battery. Figure 2 presents the propellers selected for the bench test. The tri-blade had a 4.3 pitch, and both bi-blades had a 4.5 pitch.

Table 1. Data specification and recommendations from the manufacturer.

Specification	Aeolian Outrunner Brushless Motor	T-Motor F60PRO
kv Rating (RPM/V)	1000	1750
Continuous Current (A)	22	36.11
Maximum Current (A)	28	41
Input Voltage (V)	6 – 11.1	14.8-22.69
Maximum Power (W)	390	950
Motor Dimensions (mm)	28 (Diameter) x 31 (Length)	27.5 (Diameter) x 33.5 (Length)
Motor Weight (g)	65	35.1
Manufacturer Recommended Propeller (inch)	9x4.5, 10x5, 10x6	5-inch
Application	RC Airplanes	5-inch FPV Racing Drones
Manufacturer/Supplier	Sky Team International LTD	T-MOTOR

Fig. 2. Selected propellers.

2.1.2 Prototype test architecture

The architecture of the prototype test is based on the constructed UAV. The communication system included the FLYSKY FS-i6X 2.4 GHz Radio Transmitter and FS 6CH IA6B Receiver, chosen for robust manual control. Table 2 provides the detailed specification of the propulsion system utilised in the prototype equipped with contra-rotating propellers. Figure 3 presents a visual illustration of the constructed UAV.

Table 2. Prototype's propulsion system specifications.

UAV Propulsion System	**Value/ Description**
Number of motors	(2x) T-Motor F60PRO
Fully Charged Battery Pack	3S2P LiPo (12.6V)
Electrical Speed Controller	(2x) 30 A Aeolian ESCs
Control Servos	(2x) Emax ES08MDII Servo
Flight Management Unit (FMU)	Pixhawk 2.4.8 (firmware; ArduPilot coaxial configuration)
Power Module	3DR

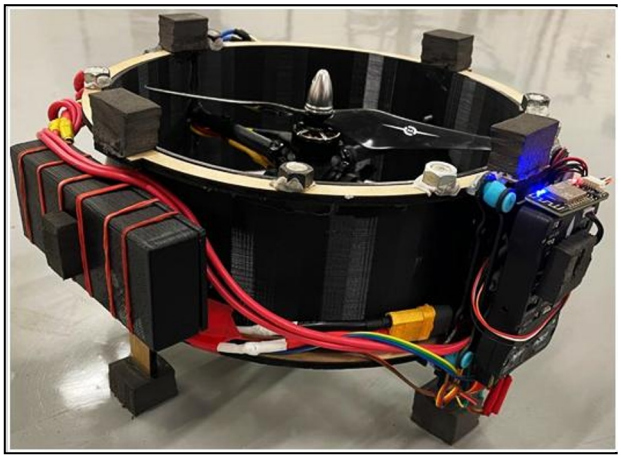

Fig. 3. The UAV utilized in the prototype test.

The *Pixhawk 2.4.8*, functioning as the FMU, has built-in sensors that act as measuring devices, providing linear acceleration, angular rate, attitude/heading, and barometric altitude. The propellers selected for the prototype varied only in pitch and blade count, because the duct was constructed to accommodate an 8-inch diameter. Figure 4 presents a visual illustration of all the propellers utilised in the prototype test.

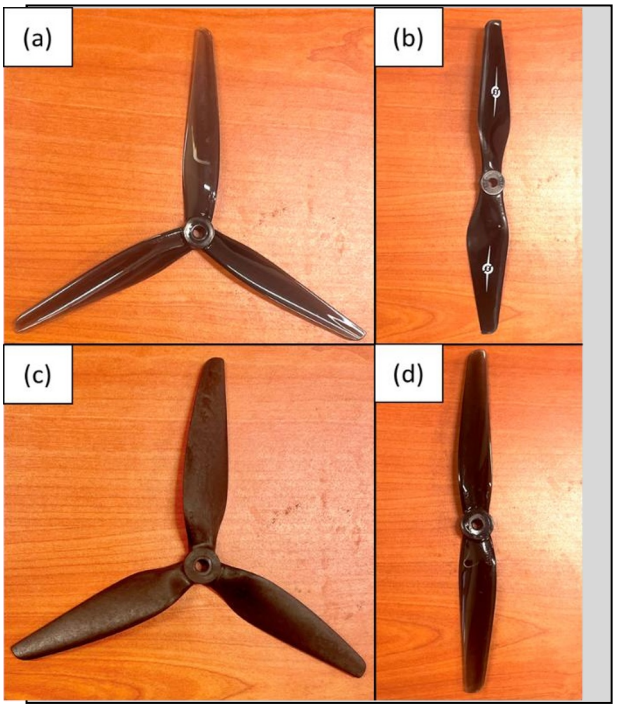

Fig. 4. All propellers: (a) HQ Prop 8 x 3.7 x 3 polycarbonate, (b) 8 x 4.5 x 2 multi-rotor series, (c) HQ Macro Quad Prop 8 x 4.5 x 3 carbon-reinforced nylon, (d) HQ Prop 8 x 5 x 2 polycarbonate.

2.2 Experimental set-up and procedure

Carefully set conditions were established to ensure the reliability of the results. All experiments were conducted in-doors on a controlled environment, to minimise random environmental variability which could influence the performance results of the propellers. For the two previously mentioned experimental setups; batteries were fully charged before commencing testing. Maintaining nominal voltage levels ensured consistency, in generating thrust.

2.2.1 Bench testing procedure

During the bench test of the three propellers shown in Figure 2, caution was exercised. The frictionless test rig was configured, and the procedure is as follows:

- A T-Motor motor was mounted onto a motor mounting plate attached to a frictionless test rig. A spring balance was calibrated and aligned with the rotary arm for accurate thrust measurement.
- A fishing line was connected to the motor mounting plate going, under the pulley, then to the spring balance, connecting the overall test rig.
- The hardware connection is shown in Figure 1. The inclusion of a digital multimeter was used when a LiPo battery (4S Nano-Platinum Series) with a voltage greater than 12 V was utilized. This condition was necessary because that is the minimum voltages required to utilize the digital multimeter.
- A dry run was conducted on the test rig without a propeller to check system functionality, gradually increasing the throttle using a servo adjustor.
- The experiments were conducted by sequentially mounting different propellers, then increasing (until peak) and decreasing the throttle, capturing thrust values with a video recording smartphone mounted in front of the rig. The propellers used were those presented in Figure 2).
- Additionally, replacing the 25A ESC with a 30A model and repeating the testing process for each propeller ensured data consistency.
- The T-Motor was swapped for an Aeolian Outrunner Brushless Motor C2830 1000 kv and replicated all previous steps to compare performance differences across motors and ESC setups. It is worth mentioning that this motor would be tested with only the 2S Turnigy LiPo battery to prevent burning it.
- Performance data was collected from the test rig, from a single load-unload cycle, captured from two angles, which were merged to synchronise the results, tabulated then visually analysed using graphs.
- The overall numerical method for obtaining propeller efficiency follows [13]. Since torque was not initially measured, a modified equation is provided in Equation 1. his equation deviates from the traditional dimensionless efficiency and should be used only to compare the generated thrust against the input power for that specific system. This step was included in tests that incorporated the digital multimeter, which displayed the power consumed for each test. The thrust-to-input-power ratio is a key performance metric in aerospace, used to assess propulsion-system efficiency, and can be compared either at a specific RPM or averaged to evaluate overall propeller performance [14].

$$\eta = \frac{Thrust}{Power} \tag{1}$$

2.2.2 Prototype testing procedure

During the UAV optimisation, the following setups and procedures were used:

- The prototype was positioned in front of the video-recording smartphone.
- Before commencing, the ESCs were calibrated. The procedure is that the UAV was armed by connecting the battery terminals and the power module terminals. Using a remote transmitter, it would vertically take off and try to archive the hovering state with the sets of propellers used.
- The experiments were conducted by increasing the thrust output of the UAV and testing different propellers with higher pitch or more blades (sets shown in Figure 4), while maintaining the same BLDC motors to keep RPM constant and voltage requirements. The selected propeller only varied in pitch and blade counts due to the size of the duct being constructed to accommodate a propeller with an 8–inch diameter.

3 Results and discussion

The two distinct experiments conducted were primarily focused on achieving the highest thrust while analysing the impact of the propellers. As previously mentioned, the tests were recorded, analysed and presented using graphs. This section presents the findings from the experiments.

3.1 Bench test

The bench test analysed thrust generated by three propellers. While manufacturers typically provide thrust estimates and recommended drivetrain configurations, these specifications often differ significantly from real-world performance. Conducting practical tests ensures more reliable data for the propulsion system. The tested propellers, differing primarily in diameter and blade count as shown in Figure 2, include an 8-inch plastic dual-blade (Prop 1), a 5-inch plastic tri-blade (Prop 2), and a 9-inch carbon fibre dual-blade (Prop 3).

Following the procedure mentioned in section 2.2.1, thrust measurements were recorded at maximum throttle using a 4S Nano-Platinum Series (14.8 V) LiPo battery. As provided in Figure 5, Prop 1 achieved the highest thrust, approximately 1700 g. This configuration was based on the use of a T-Motor F60PRO V.20 kv 1750 BLDC motor, connected with a 30 A ESC. The configuration must have struck a balance between component safety and optimal performance, as confirmed by the recorded data. When using the 25 A ESC, the results were slightly lower when compared with those of the 30A ESCs. However, Prop 1 still generated the highest possible thrust from configuration, approximately 1550 g. In both configurations, Prop 3 tend to vibrate, and at some instant even overheat the motor. This may be attributed to the diameter size being almost 2x the recommended size.

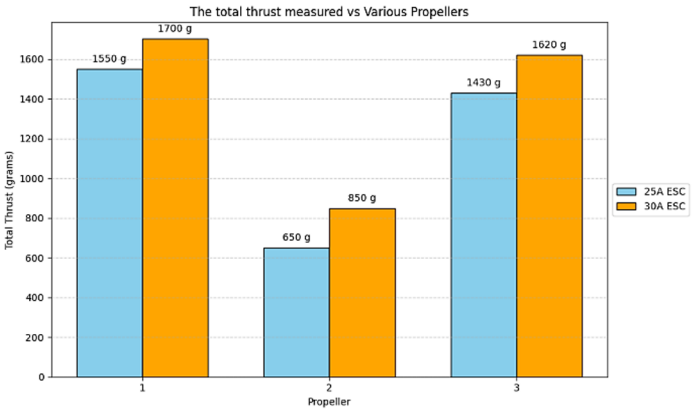

Fig. 5. The compared thrust measurements for the sets of propellers over T-Motor F60PRO V.20 kv 1750.

The 2S Turnigy (7.4 V) LiPo battery was used for the Aeolian Outrunner Brushless Motor C2830 1000 kv, which has a lower voltage requirement. Figure 6 shows that at peak throttle, the 25 A ESC achieved the highest thrust of 220 g with Prop 3. However, the 25 A ESC experienced rapid heat buildup due to the load imposed by these propellers, indicating the need for better thermal management for sustained operations. The 30 A ESC experienced the highest thrust for the Prop 3 configuration.

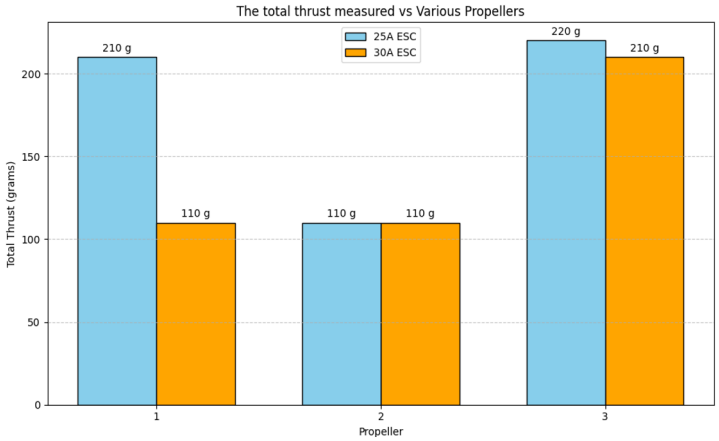

Fig. 6. The compared thrust measured the sets of propellers over Aeolian Outrunner Brushless Motor C2830 1000 kv.

From the experiments presented above, the most efficient configurations for maximizing thrust while ensuring component safety was identified as the T-Motor F60PRO V2 1750 kv, paired with a 30 A Aeolian ESC and powered by a 4S Nano-Platinum Series (14.8 V) battery. Figure 7 presents the displayed power vs thrust from the tests, and Figure 8 provides the overall propeller efficiency, using equation 1. The Aeolian motor on a 30 A ESC with 5-inch could not lift the support arm due to the required power. Hence those results were not included in the presents graphs.

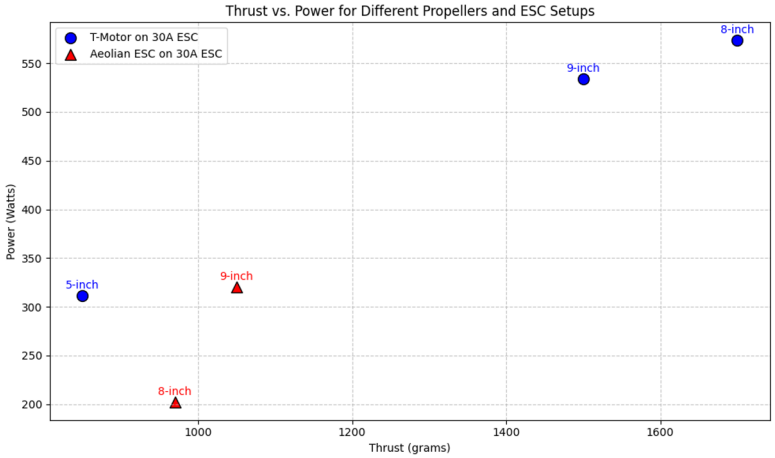

Fig. 7. Compared thrust over power measured from different propeller.

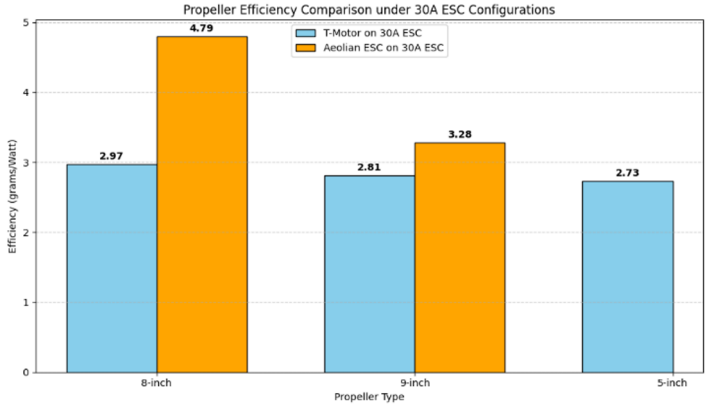

Fig. 8. Overall efficiency.

3.2 Prototype test

The previous experiment test also informed the design specifications for the UAV prototype, constraining the duct to accommodate 8-inch propellers mounted on the T-Motor F60PRO V2 1750 Kv. Once fabricated, the prototype's performance required optimization. One recommendation focused on increasing thrust output using propellers with a higher pitch or greater blade count while maintaining the same BLDC motors to ensure constant RPM.

Since thrust data in newtons or grams were not available on flight logs during prototype testing, the maximum altitude obtained (as observed visually and through logs) and corresponding voltage readings at full throttle were analysed. Hence in this context with airframe mass, motors, and battery held constant, and propeller being the changing variable a higher full-throttle altitude indicates a larger net thrust margin overweight (i.e., a higher thrust-to-weight ratio) and therefore better vertical performance for the VTOL prototype. After several tests, as shown in Figure 9, the least compatible propeller was identified as (A) HQ Prop 8 x 3.7 x 3. Despite having three blades, its low pitch resulted in the UAV barely achieving lift-off, reaching a maximum altitude of only 0.63 meters. In contrast, the HQ Prop

8 x 5 x 2 polycarbonate significantly enhanced performance, achieving higher altitudes of approximately 2.09 meters.

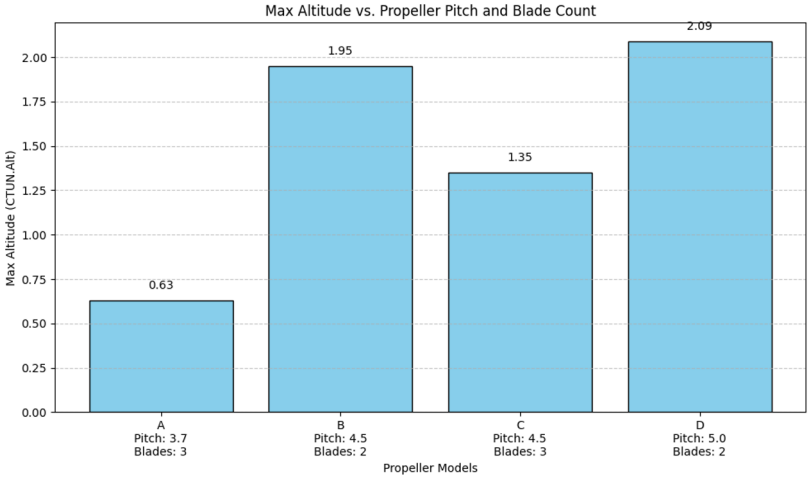

Fig. 9. Maximum altitude reached through the propeller models.

Figure 10 presents the different voltage readings for the propellers tested at peak altitudes. As (A) HQ Prop 8 x 3.7 x 3 barely took off, it was clear that the low pitch of the propeller consumes more voltage. It oscillates on the ground and can contribute to excessive voltage consumption, thus obtaining the highest voltage drop. The HQ Prop 8 x 5 x 2 polycarbonate had the highest second voltage drop, though its pitch allowed it to reach a higher altitude, it was however not as efficient. From the reading propellers B and C had the same pitch differing in blade count showing that, increasing the number of blades on the propeller may increase the voltage consumption.

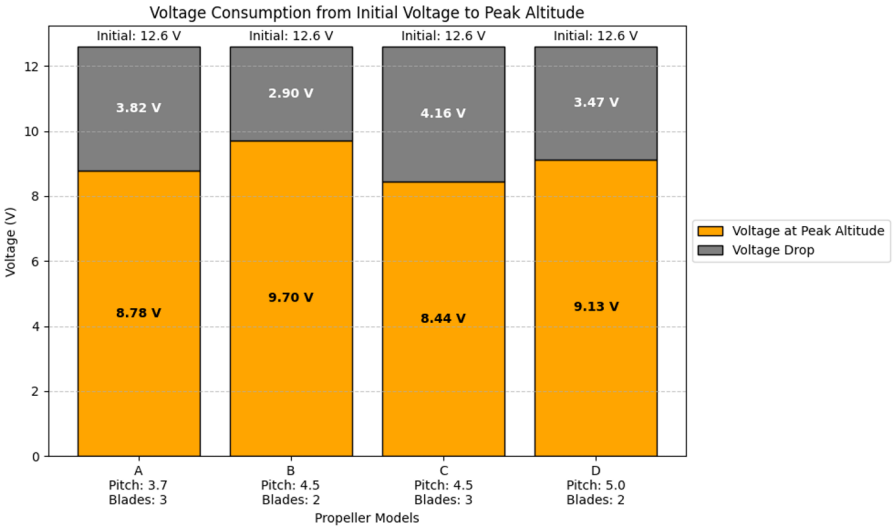

Fig. 9. Voltage distribution across propeller models.

4 Conclusion

This study presented a practical and comprehensive method for analysing and optimising propeller configurations in UAV propulsion systems. Essential to the study was the design and implementation of a low-cost, in-house-fabricated frictionless test rig, which enabled systematic evaluation of the effects of propeller diameter, pitch, and blade count on thrust, efficiency, and power consumption. By integrating BLDC motors, ESCs, and LiPo batteries, this experimental setup replicated real-world UAV operating conditions, ensuring results were both relevant and actionable.

The approach offered a number of advantages. Unlike resource-intensive setups such as wind tunnels, the proposed methodology relied on easily accessible materials PVC pipes, 3D-printed components, and a commercial spring balance making it highly replicable and adaptable for researchers with limited resources. This setup allowed for controlled variation of individual propeller parameters, providing insights not only into individual component behaviour but also into their combined effects on propulsion performance.

Implementation of this methodology led to several significant outcomes. Firstly, the bench test identified that the T-Motor F60PRO V2 1750 kv motor, paired with a 4S Nano-Platinum Series (14.8 V) LiPo battery and an 8-inch dual-blade propeller (Prop 1), achieved the highest thrust (~1700 g), offering an optimal configuration for maximum thrust while maintaining component safety. Secondly, the prototype tests validated these findings and further explored the impact of pitch and blade count. The HQ Prop 8 x 5 x 2 polycarbonate propeller delivered the highest altitude (~2.09 m), although the HQ Prop 8 x 4.5 x 2 polycarbonate showed the best balance between thrust, and voltage efficiency.

In terms of research contributions, this study:

- Developed a replicable, low-cost frictionless test rig: This was constructed using recycled and additive-manufactured components, offering a novel yet practical alternative to more complex systems.

- Systematically analysed propeller parameters: Blade diameter, pitch, and count were individually varied under consistent testing conditions, allowing for isolated performance evaluations.

- Validated optimal configurations through prototype testing: Insights from bench tests informed the prototype design, which was further optimised through controlled flight experiments using multiple propeller variations.

- Provided a comparative framework bridging theory and practice: Real-world data often diverges from manufacturer claims; this study offered empirically grounded results to guide future UAV propulsion design decisions.

Future work will enhance the test rig with integrated torque, real-time power, and motor-temperature sensing; investigate advanced propeller materials and adaptive-pitch mechanisms; and submit datasets to benchmarking platforms (e.g., RC Benchmark). In addition, we will document the lubrication approach and implement a plan to quantify residual hinge friction to improve testing and aid replication; Figure 1 illustrates a schematic layout of the constructed test rig. The campaign will extend beyond single-propeller tests to quantify coaxial/contra-rotating effects (varying spacing and rotation sense), improve force

measurement using a digital "fishing scale" and/or a calibrated load cell, and enable cross-session comparison by logging temperature, pressure, and humidity and normalising for air density. Each propeller will undergo repeated load–unload cycles (reporting mean ± s.d. and checking for hysteresis), and the prototype will be evaluated with tethered thrust measurements to obtain direct thrust–power curves and reduce confounding effects.

The author would like to sincerely thank Riaan Stopforth, Daniel Kirkman, and Maxim Buzdalov for their invaluable guidance, support, and expertise throughout this study. The author also gratefully acknowledges the financial support provided by the CSIR Bursary Programme; without it this work would not have been possible.

Data availability. Data is available on request due to privacy/ethical restrictions.

References

[1] H. Zhang, B. Song, F. Li, and J. Xuan, "Multidisciplinary design optimization of an electric propulsion system of a hybrid UAV considering wind disturbance rejection capability in the quadrotor mode," Aerosp Sci Technol, vol. 110, Mar. 2021, doi: 10.1016/j.ast.2020.106372.

[2] J. A. Prakosa, D. V. Samokhvalov, G. R. V. Ponce, and F. Sh. Al-Mahturi, "Speed Control of Brushless DC Motor for Quad Copter Drone Ground Test," in 2019 IEEE Conference of Russian Young Researchers in Electrical and Electronic Engineering (EIConRus), IEEE, Jan. 2019, pp. 644–648. doi: 10.1109/EIConRus.2019.8656647.

[3] B. Stiltner, J. Faber, C. Olien, R. Merritt, and S. Tanious, "Detailed Design, Construction, and Flight Tests of a Remotely Piloted Ducted Fan MAV," in 48th AIAA Aerospace Sciences Meeting Including the New Horizons Forum and Aerospace Exposition, Reston, Virigina: American Institute of Aeronautics and Astronautics, Jan. 2010. doi: 10.2514/6.2010-1021.

[4] R. Nederlof, D. Ragni, and T. Sinnige, "Experimental Investigation of the Aerodynamic Performance of a Propeller at Positive and Negative Thrust and Power," in AIAA AVIATION 2022 Forum, Reston, Virginia: American Institute of Aeronautics and Astronautics, Jun. 2022. doi: 10.2514/6.2022-3893.

[5] K. Baskaran, N. S. Jamaluddin, A. Celik, D. Rezgui, and M. Azarpeyvand, "Effects of number of blades on propeller noise," J Sound Vib, vol. 572, p. 118176, Mar. 2024, doi: 10.1016/j.jsv.2023.118176.

[6] D. Felix Finger, C. Braun, and C. Bil, "A Review of Configuration Design for Distributed Propulsion Transitioning VTOL Aircraft," 2017.

[7] M. El Adawy et al., "Design and fabrication of a fixed-wing Unmanned Aerial Vehicle (UAV)," Ain Shams Engineering Journal, vol. 14, no. 9, p. 102094, Sep. 2023, doi: 10.1016/j.asej.2022.102094.

[8] A. Filippone, "Historical development of the coaxial contra-rotating propeller," The Aeronautical Journal, vol. 127, no. 1311, pp. 699–736, May 2023, doi: 10.1017/aer.2022.92.

[9] B. Hasilci and T. V. Mumcu, "Parameter Estimation of BLDC Motors by SVM for UAV Propulsion Systems," Erzincan Üniversitesi Fen Bilimleri Enstitüsü Dergisi, vol. 15, no. 2, pp. 406–419, Aug. 2022, doi: 10.18185/erzifbed.930222.

[10] U. F. Ukaegbu, L. K. Tartibu, M. O. Okwu, and I. O. Olayode, "Development of a Light-Weight Unmanned Aerial Vehicle for Precision Agriculture," Sensors, vol. 21, no. 13, p. 4417, Jun. 2021, doi: 10.3390/s21134417.

[11] S. Atoev, O. H. Kwon, S. H. Lee, and K. R. Kwon, "An efficient SC-FDM modulation technique for a UAV communication link," Electronics (Switzerland), vol. 7, no. 12, Dec. 2018, doi: 10.3390/electronics7120352.

[12] H. Cai, Z. Zhang, and S. Deng, "Numerical Prediction of Unsteady Aerodynamics of a Ducted Fan Unmanned Aerial Vehicle in Hovering," Aerospace, vol. 9, no. 6, Jun. 2022, doi: 10.3390/aerospace9060318.

[13] Z. Zhang, Y. Zhang, J. Yu, P. Du, and J. Zhao, "Variable Pitch Propeller: Multi-Objective Optimization Design and Performance Analysis," in 2nd International Conference on Green Aviation (ICGA 2024), Basel Switzerland: MDPI, Feb. 2025, p. 36. doi: 10.3390/engproc2024080036.

[14] A. Pugna, C. Hrab, L.-N. Hînsa, A. Hopârtean, C.-M. Giurgea, and L. Marcu, "Development of an experimental setup for propeller performance measurements," E3S Web of Conferences, vol. 608, p. 02013, Jan. 2025, doi: 10.1051/e3sconf/202560802013.